



# Large variations in Holocene solar activity: Constraints from $^{10}\text{Be}$ in the Greenland Ice Core Project ice core

Maura Vonmoos,<sup>1</sup> Jürg Beer,<sup>1</sup> and Raimund Muscheler<sup>2</sup>

Received 26 October 2005; revised 1 June 2006; accepted 17 July 2006; published 12 October 2006.

[1] Cosmogenic radionuclides extracted from ice cores hold a unique potential for reconstructing past solar activity changes beyond the direct instrumental period. Taking the geomagnetic modulation into account, the solar activity in terms of the heliospheric modulation function can quantitatively be reconstructed in high resolution throughout the Holocene. For this period our results reveal changes in heliospheric modulation of galactic cosmic rays significantly larger than the variations reconstructed on the basis of neutron monitor measurements of galactic cosmic rays for the last 50 years. Moreover, the  $^{10}\text{Be}$  data from the Greenland Ice Core Project ice core as well as  $^{14}\text{C}$  support a high current solar activity. However, although the reconstruction of solar activity on long timescales is difficult, our result suggests that the modern activity state of the Sun is not that exceptional regarding the entire Holocene. This extended solar activity record provides the basis for further detailed investigations on solar and cosmic ray physics, as well as on solar forcing of the Earth's climate whose importance is suggested by increasing paleoclimatic evidences.

**Citation:** Vonmoos, M., J. Beer, and R. Muscheler (2006), Large variations in Holocene solar activity: Constraints from  $^{10}\text{Be}$  in the Greenland Ice Core Project ice core, *J. Geophys. Res.*, **111**, A10105, doi:10.1029/2005JA011500.

## 1. Introduction

[2] Various observations of solar parameters over the last decades to centuries have revealed that the Sun is a variable star. Since 1951, neutron monitors have been recording variations in galactic cosmic rays (GCR) entering the Earth's atmosphere which are attributable to changes in heliospheric modulation [Beer, 2000b; Masarik and Beer, 1999; Simpson, 1978; Usoskin *et al.*, 2002]. For about the past 30 years, satellite-based radiometers have shown variations of the total solar irradiance, which is still misleadingly named "solar constant." However, the measured variability in the total solar irradiance is small. The amplitude over a typical 11-year solar cycle is only about 0.1% [Fröhlich, 2006; Fröhlich and Lean, 1998; Willson, 1997]. Monitoring of other stars over the past approximately 20 years, on the other hand, has partly revealed significantly larger variations in their brightness [Baliunas and Jastrow, 1990; Lockwood, 1994; Radick *et al.*, 1990]. Though their primarily assumed similarity to the Sun is questioned in recent studies [Hall and Lockwood, 2004], larger variations on longer timescales than observed so far cannot be excluded either for the Sun. This is indeed indicated by historical solar observations covering up to 4 centuries. They clearly point to a solar magnetic variability larger than observed during the satellite-based radiometry and the neu-

tron monitoring period. The longest direct record of solar magnetic activity starts at 1610 AD and has been obtained from observations of the Sun's surface, in particular the occurrence of sunspots (first continuous reconstruction by Rudolf Wolf) or sunspot groups [Hoyt and Schatten, 1998]. Superimposed on the well-expressed 11-year solar cycle, the so-called Schwabe cycle, are larger long-term variations (i.e., grand solar minima [Eddy, 1976]). Since the Maunder Minimum (1645–1715 AD), when hardly any sunspots were observed, the average solar activity as manifested by sunspots has generally increased, interrupted by temporarily drops around 1800 AD (Dalton Minimum) and at the end of the 19th century. Further evidence of a larger magnetic solar variability on decadal to centennial timescale than observed over the last 50 years are obtained from measurements of other magnetic activity proxies such as the geomagnetic *aa* index [Lockwood, 2004; Mayaud, 1973], the occurrence of aurora [Legrand and Simon, 1987] as well as from the solar radius [Ribes *et al.*, 1991] although the latter is still debated. Their consistent 11-year cycle confirms these different proxies in being physical manifestations of the magnetic activity of the Sun, even though differently related both to the solar magnetic field and among them. However, the instrumental measurement period is limited to the last few decades to centuries, depending on the particular observed solar index and their reliability generally decreases with age.

[3] Knowledge of the total bandwidth of our Sun's variability is widely required, especially in the field of solar and cosmic ray (CR) physics and (paleo)climatology. On the part of solar physics, this knowledge can improve the understanding of solar magnetic activity, i.e., the solar

<sup>1</sup>Swiss Federal Institute of Environmental Science and Technology, Dübendorf, Switzerland.

<sup>2</sup>Climate and Radiation Branch, NASA Goddard Space Flight Center, Greenbelt, Maryland, USA.

dynamo generating the solar magnetic field in the Sun's convective zone and the physical processes inducing the temporal and spatial variations in its magnetic strength. A prolonged solar record spanning several thousands of years provides important insights into the solar activity's cyclic nature and recurrent temporary persistence in modes of constantly reduced magnetic activity, the so-called grand solar minima. In CR physics, a classical task is the propagation of GCR through the heliosphere and its variability related to solar magnetic activity. The heliosphere extends to about 120 astronomical units (AU) into space and is filled by the open solar magnetic flux, the solar magnetic field frozen in the solar wind streaming out of the Sun's surface. Knowledge of long-term solar modulation of the GCR flux can indirectly extend the existing 50 years long neutron monitor records of GCR significantly [Beer, 2000b; McCracken, 2001, 2004; McCracken and McDonald, 2001]. This allows studying GCR and processes associated with the heliospheric modulation of GCR on longer time-scales than what has been possible on the basis of neutron monitor data.

[4] Furthermore, the Sun is by far the most important energy source for the Earth's climate system. With the discovery of the Sun's variability increasing interest has been directed toward its significance as a variable natural climate forcing factor [Eddy, 1976; Lean et al., 1995; Lean and Rind, 1999; Reid, 1991; Rind, 2002]. There is a growing number of paleoclimatic studies pointing toward a strong solar forcing on past climate [Bond et al., 2001; Denton and Karlén, 1973; Fleitmann et al., 2003; Hodell et al., 2001; Magny, 1993; Neff et al., 2001; Van Geel et al., 1996; Verschuren et al., 2000]. Therefore a long and quantitative record of past solar activity is of special interest for paleoclimatologists and climate modelers to determine the Sun's potential of variability and to assess possible future activity ranges. The relevant form of solar impact on the climate is its total and spectral irradiance, especially the UV [Haigh, 1994, 1996, 1999; Shindell et al., 2001]. Since total solar irradiance changes correlate well with weak solar magnetic field changes during the instrumental period, a long-time record of solar activity as manifested by the open fields holds a large potential for reconstructing long-term solar irradiance variability.

[5] Owing to the lack of complete direct observations of the Sun for the period before AD 1600, one has to rely on indirect sources of information to acquire knowledge about the Sun's long-term behavior and total extent of variability. One of the most reliable indirect proxies of solar variability are represented by cosmogenic radionuclides, such as  $^{14}\text{C}$  and  $^{10}\text{Be}$  or  $^{36}\text{Cl}$ , that can be determined with high resolution from tree ring and ice core archives reaching back in time ten and hundreds of thousands of years, respectively [Baumgartner et al., 1997a; Finkel and Nishiizumi, 1997; Muscheler et al., 2004; Stuiver et al., 1998; Wagner et al., 2001; Yiou et al., 1997]. However, the extraction of the solar signal from cosmogenic radionuclide records is not straightforward, since they are influenced by different components (see section 3). Yet, cosmogenic radionuclides turned out to be particularly suitable for extending the record of past solar variability [Beer, 2000a]. Various reconstructions of solar activity for the last millennium or the entire Holocene are based on them, so in terms of

total solar irradiance [Bard et al., 2000] and sunspots [Solanki et al., 2004; Usoskin et al., 2003]. In this paper we present a different method to Usoskin et al. [2003] to reconstruct solar variability quantitatively in terms of the solar modulation function using the cosmogenic radionuclide  $^{10}\text{Be}$ . Spanning around 9000 years, this record provides an unprecedented basis for the detailed discussion of relevant questions regarding solar and CR physics, as well as the solar forcing of the Earth's climate system.

## 2. Solar Modulation Function $\Phi$

[6] The production rate of cosmogenic radionuclides depends on the intensity of GCR penetrating the Earth's atmosphere. Before reaching the Earth, GCR have to cross the heliosphere where they are subject to solar induced modulation effects. The propagation of GCR through the heliosphere is described by the cosmic ray transport equation formulated by Parker [1965]. In this formula the following processes are taken into account [Caballero-Lopez and Moraal, 2004]: (1) pitch angle scattering of the particles along the magnetic field lines; (2) diffusion perpendicular to the field lines; (3) gradient curvature, neutral sheet, and shock drift effects; (4) convection in the solar wind; (5) adiabatic energy gains; and (6) adiabatic energy losses in the expanding solar wind.

[7] The Parker transport equation can only be numerically solved and requires a detailed knowledge of the cosmic ray intensity as a function of the three spatial coordinates, time, and energy. To reduce the complexity, several simplifying assumptions have been introduced such as [McCracken et al., 2004]: (1) the heliosphere is spherically symmetric and in a quasi-steady state; (2) the net streaming of GCR is negligible compared to diffusion; (3) the diffusion coefficients can be separated into a function of distance from the Sun and a function of the rigidity (momentum to charge ratio) of the cosmic rays. On the basis of these assumptions, Gleeson and Axford [1968] derived the so-called force-field equation:

$$J(E_P) = J_{\text{LIS}}(E_P + \Phi) \frac{E_P(E_P + 2m_p c^2)}{(E_p + \Phi)(E_p + 2m_p c^2 + \Phi)} \quad (1)$$

where  $J_{\text{LIS}}$  is the local interstellar cosmic ray flux, that is, the flux of GCR particles outside the heliosphere,  $E_P$  is the proton's kinetic energy [MeV],  $\Phi$  is the solar modulation function [MeV],  $c$  is the velocity of light, and  $m_p c^2$  is the proton's rest energy = 938 MeV.

[8] This equation relates the GCR intensity with energy  $E_P$  at the distance 1 AU (Astronomical Unit =  $149.6 \times 10^6$  km) from the Sun,  $J(E_P)$ , to the GCR intensity with energy  $E_P + \Phi$  in the local interstellar region,  $J_{\text{LIS}}(E_P + \Phi)$ . The modulation function  $\Phi$  quantifying formally an energy loss, changes the shape of the differential energy spectrum of GCR particles. The degree of this change diminishes with increasing energy  $E_P$  (Figure 1).  $\Phi$  can be expressed by the modulation potential  $\phi(r, t)$ :

$$\Phi = Ze\phi(r, t) \quad (2)$$

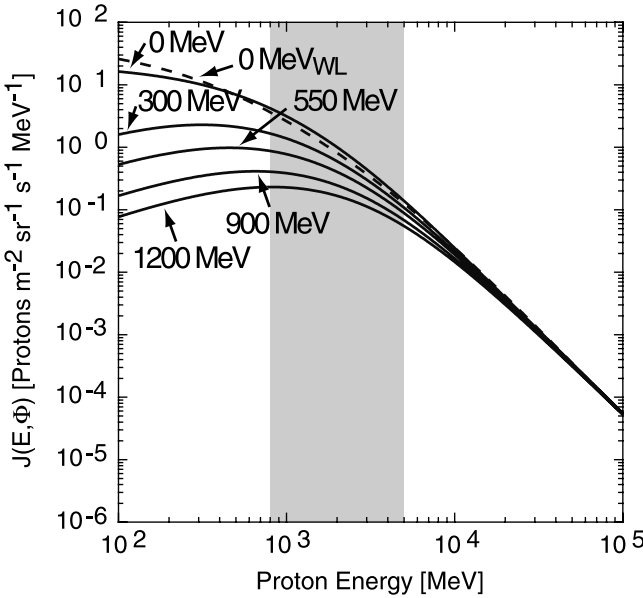


**Figure 1.** Energy spectra of the primary galactic cosmic ray (GCR) proton flux at 1 AU for different values of the solar modulation function  $\Phi$ . The spectra are calculated using the force-field approximation [Gleeson and Axford, 1968] of the transport equation and the local interstellar spectrum of GCR protons published by Cini Castagnoli and Lal [1980], equations (1) and (4). The curves are labeled with the value of the corresponding solar modulation function  $\Phi$ . While the spectra for  $\Phi$  values above 300 MeV are supported by measurements [Cini Castagnoli and Lal, 1980], the others cannot be verified by experimental data so far. The curve labeled with  $\Phi = 0$  MeV corresponds to the local interstellar flux, that is, the estimated flux of GCR particles outside the heliosphere. A new approximation of the local interstellar spectrum of Webber and Lockwood [2001] (dashed curve,  $\Phi = 0$  MeV<sub>WL</sub>) shows only small differences to the spectrum of Cini Castagnoli and Lal [1980], especially in the energy range which is important for the radionuclide production (gray bar) [Webber and Higbie, 2003].

where  $Ze$  is the electrical charge of the particle. Here  $\phi(r,t)$  is related to the solar wind speed  $V(r,t)$  and the diffusion coefficient  $\kappa(r,t)$  of the GCR in the heliomagnetic field:

$$\phi(r,t) = \int_r^{r_b} \frac{V(r,t)}{3\kappa(r,t)} dr \quad (3)$$

where  $r$  is the distance from the Sun and  $r_b$  is the outer boundary of the heliosphere. The modulation function  $\Phi$  that describes the adiabatic energy loss of the GCR is measured in MeV, whereas the energy loss per unit charge  $\phi$  is quoted in MV.

[9] Caballero-Lopez and Moraal [2004] have investigated different approximations by comparing them with the full numerical solution of the Parker transport equation. They have found that at the distance of 1 AU and for energies  $E_p > 500$  MeV the force-field approximation works well and leads to good empirical fits with observed cosmic ray spectra [Webber and Lockwood, 2001].

[10] From equation (1) it is obvious that the GCR spectra and correspondingly the production rate of cosmogenic radionuclides depends on the local interstellar cosmic ray flux  $J_{LIS}$  and its modulation by  $\Phi$ . The differential energy spectra used in our work and shown in Figure 1 as a function of the solar modulation function  $\Phi$  are based on the local interstellar spectrum of Cini Castagnoli and Lal [1980]:

$$J_{LIS} = C_P (E_p + x)^{-2.65} \quad (4)$$

where  $x = 780 \exp(-2.5 \times 10^{-4} E_p)$  and  $C_P = 1.244 \times 10^6 \text{ cm}^{-2} \text{ s}^{-1} \text{ MeV}^{-1}$  is the normalization factor.

[11] While most authors use the same force-field approximation as we do [McCracken et al., 2004; Webber and Higbie, 2003], the  $J_{LIS}$  has been modified recently based on new instrumental data acquired by spacecrafts in the outer heliosphere where solar modulation is weak [Webber and Lockwood, 2001]. However, Figure 1 shows that the difference to our work [Cini Castagnoli and Lal, 1980; Masarik and Beer, 1999] is smaller than 10% in the energy range where the  $^{10}\text{Be}$  response to GCR is largest (gray bar in Figure 1) [McCracken, 2001, 2004; Webber and Higbie, 2003].

[12] Figure 1 illustrates the enhanced shielding effect during periods of high solar activity, that is, the enhanced energy loss of the GCR protons due to the increased intensity of the magnetic field carried in the solar wind. For a given change in  $\Phi$  the effect on the GCR proton flux intensity is largest for periods of small solar activity.

[13] The effect of the solar modulation increases strongly toward lower energies, and this coincides with the most efficient energy range for the subsequent production of the cosmogenic radionuclide  $^{10}\text{Be}$  from GCR in the Earth's atmosphere, which is around 1–2 GeV [McCracken, 2001, 2004; Webber and Higbie, 2003]. This shows that  $^{10}\text{Be}$  time series can be used as sensitive recorders of past solar modulation and thus of the temporal variability of the open solar magnetic field, especially in periods of low solar activity.

[14] The modulation function  $\Phi$  provides, like the different manifestations of solar activity, only one specific aspect of solar magnetic activity with not yet fully understood relation to the ongoing magnetic processes in and on the surface of the Sun. The comparison of the two widely used solar magnetic activity proxies, the  $^{10}\text{Be}$  production rate (depending on heliomagnetic modulation of GCR by the open magnetic field from the Sun and related to coronal mass ejections) and the sunspot group number (reflecting strong magnetic flux tubes crossing the photosphere), reveals distinct differences in their sensitivity to record changes in the solar activity. In the 11-year solar cycle minima the number of sunspots is close to zero and cannot differentiate between the different strengths of the minima, whereas the  $^{10}\text{Be}$  production rate does. This important difference is obvious during the Maunder Minimum when the  $^{10}\text{Be}$  record from the Dye3 ice core continuously shows an 11-year solar cycle, whereas almost no sunspots were observed [Beer et al., 1998]. This may indicate a threshold level of solar activity for the appearance of sunspots and thus that a sunspot number of zero does not manifest a solar activity as low as a  $\Phi$  value of 0 MeV does.

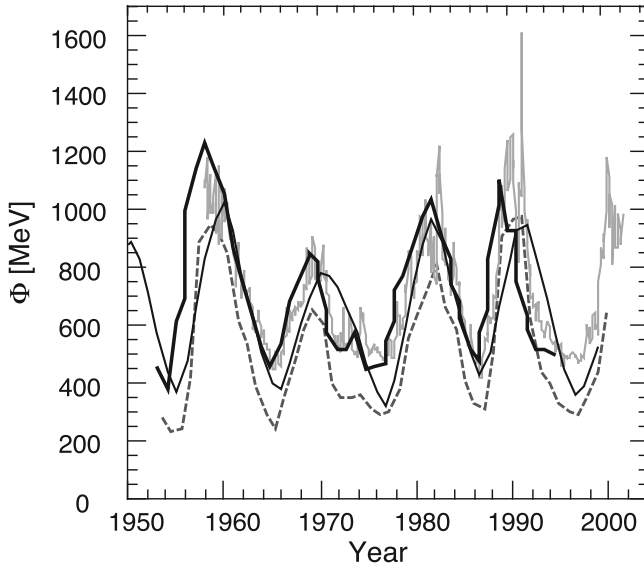


**Figure 2.** Comparison of different  $\Phi$  estimates for the past 50 years. Three  $\Phi$  reconstructions are based on neutron monitor counting rates measured by different neutron monitors, see the specific references for details. Bold black line: *Masarik and Beer* [1999]; dashed gray line: *Usoskin et al.* [2002]; light gray solid line:  $\Phi$  data from FAA (see text), <http://www.cami.jccbi.gov/AAM-600/Radiation/600radio.html>. The  $\Phi$  after *Bonino et al.* [2001] (thin black line) is calculated on the basis of his reconstructed GCR flux for the kinetic energy intervals 400–800 MeV [see *Bonino et al.*, 2001, equation (1)].

[15] For about the past 50 years,  $\Phi$  can be reconstructed by means of neutron monitor data recording the GCR particles on the Earth's surface with high precision and high temporal resolution (Figure 2). The various  $\Phi$  records show a consistent 11-year cycle but differ in their absolute values depending on the reconstruction method. Over an 11-year cycle during the neutron monitor era the reconstructed annual  $\Phi$  varied between about 450 MeV and 1200 MeV [*Masarik and Beer*, 1999], 251 MeV and 980 MeV [*Usoskin et al.*, 2002], and about 480 MeV and 1110 MeV (from The Federal Aviation Administration (FAA), <http://www.cami.jccbi.gov/AAM-600/Radiation/600radio.html>), with a mean value for three successive 11-year cycles (between 1958 and 1990) of  $\sim 710$  MeV,  $\sim 540$  MeV, and  $\sim 720$  MeV, respectively (Figure 2). An annual  $\Phi$  record, calculated using the 300 years long GCR spectra inferred by *Bonino et al.* [2001], varied between about 430 MeV and 1130 MeV with a mean value of  $\sim 750$  MeV for the above considered three 11-year cycles. For extended periods of constant low solar activity like the Maunder Minimum, in which almost no sunspots were observed, *Cini Castagnoli and Lal* [1980] assume a  $\Phi$  value of about 100 MeV. On the basis of the GCR spectra of *Bonino et al.* [2001] a minimal annual  $\Phi$  value of about 70 MeV results for the last part of the Maunder Minimum. *McCracken et al.* [2004] reconstructed a  $\Phi$  record for the past 1100 years by using  $^{10}\text{Be}$  data from South Pole revealing minimal 22-year average  $\Phi$  values of  $\sim 84$  MeV during the Oort (1010–1050 AD), Spörer (1415–1535 AD),

and Maunder Minima and  $\sim 200$  MeV during the Wolf (1280–1340 AD) and Dalton Minima. A new 1000 years long  $\Phi$  reconstruction of *Muscheler et al.* [2005b] by using  $^{14}\text{C}$  data also results in grand solar minima mean  $\Phi$  values of about 100–250 MeV. A long-term average solar modulation function over a few millions of years was reconstructed by *Masarik and Reedy* [1994] to a value of  $\Phi = 550$  MeV based on cosmogenic radionuclide data in lunar samples.

### 3. Cosmogenic Radionuclide $^{10}\text{Be}$

[16]  $^{10}\text{Be}$  is produced in the Earth's atmosphere by the interaction of GCR particles with nitrogen and oxygen [*Lal and Peters*, 1967; *Masarik and Beer*, 1999]. Owing to the shielding effect of the heliomagnetic field, as discussed in the previous section, fewer cosmogenic radionuclides are produced during periods of high solar activity than during periods of low solar activity. In addition to this heliospheric modulation, the charged GCR particles are deflected by the Earth's magnetic field depending on its strength. As the geomagnetic modulation is mainly due to the dipole field, the shielding effect is highly dependent on geomagnetic latitude, being maximal at low latitudes. The production rate of cosmogenic radionuclides as a function of geomagnetic and heliospheric modulations is well understood. Using the GCR primary proton spectra based on the force-field approximation [*Gleeson and Axford*, 1968] and on *Cini Castagnoli and Lal's* [1980] local interstellar spectrum, *Masarik and Beer* [1999] simulated the production rate of cosmogenic radionuclides by Monte Carlo techniques for each point in the atmosphere depending on different geomagnetic dipole moments and solar modulation functions  $\Phi$ . An example of their calculations is shown in Figure 3. Since they take alpha and heavier particles into account by a correspondingly larger proton flux, they slightly underestimate the heliospheric and geomagnetic modulation. However, the estimated differences are smaller than 10% for the chosen atmospheric mixing model. Therefore their results are in agreement with recent independent production rate calculations of *Webber and Higbie* [2003] using the new GCR spectra of *Webber and Lockwood* [2001], especially as far as the relative changes are concerned.

[17] Subsequent to the production,  $^{10}\text{Be}$  becomes quickly attached to aerosols and follows their pathways. After a mean residence time of 1–2 years in the atmosphere [*Raisbeck et al.*, 1981]  $^{10}\text{Be}$  is removed mainly by wet deposition and, e.g., stored in natural archives like ice caps. The  $^{10}\text{Be}$  concentration of an ice sample is thus composed of a production signal (modulated by solar and geomagnetic shielding) and of a climate system signal (atmospheric mixing, transport, and deposition). All these factors have to be considered when reconstructing the solar activity based on the  $^{10}\text{Be}$  concentrations measured in the polar ice caps. From now on, we will use the term “system effects” for all the effects on the  $^{10}\text{Be}$  concentration which are not related to the production process.

[18] As both the production of cosmogenic radionuclides and the solar modulation function  $\Phi$  are directly related to the open magnetic flux and other properties of the solar wind (equation (3) and *Caballero-Lopez et al.* [2004]),  $\Phi$  is consequently the parameter that connects solar activity most directly to the  $^{10}\text{Be}$  records. All the more so because the

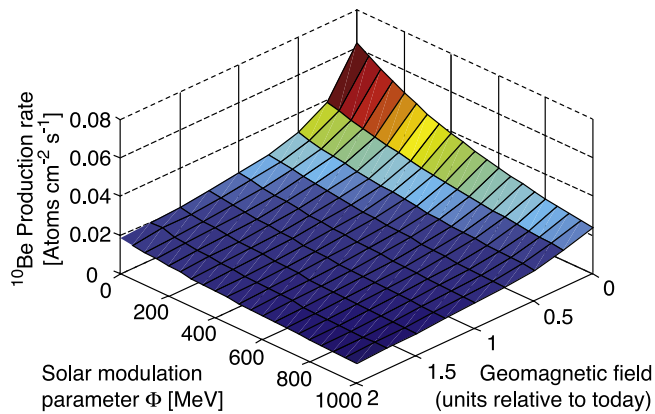


**Figure 3.** Dependence of the  $^{10}\text{Be}$  production rate on the solar activity  $\Phi$  and on the intensity of the geomagnetic field [Masarik and Beer, 1999] considering a production area covering the entire hemisphere in the stratosphere but only geographic latitudes higher than  $40^\circ$  in the troposphere. A  $\Phi$  value of 0 MeV corresponds to a quiet Sun, a  $\Phi$  value of 1000 MeV to a very active Sun. The geomagnetic field is given in relative units where the present field intensity has a value of 1. Note the highly nonlinear relationship between the  $^{10}\text{Be}$  production rate and both, the heliospheric and the geomagnetic modulation.

physical link between  $^{10}\text{Be}$  and  $\Phi$  is well understood. For the reconstruction of the other parameters of solar activity from cosmogenic radionuclides additional sophisticated physical models are required, which do not exist in most cases yet.

#### 4. $^{10}\text{Be}$ Record From the Greenland Ice Core Project (GRIP) Ice Core

[19] The  $^{10}\text{Be}$  record was measured in the 3029 m long Greenland Ice Core Project (GRIP) ice core (Summit, Central Greenland) covering several hundred thousand years [Baumgartner et al., 1997b; Muscheler et al., 2004; Wagner et al., 2001; Yiou et al., 1997]. We use the timescale published by Johnsen et al. [1997] (ss09 timescale).  $^{10}\text{Be}$  concentration measurements corresponding to the Holocene are available from 304 to 9315 years BP. As for all deep drilling ice cores, the top part of the GRIP ice core is lacking for technical reasons. Being dependent on the depth, the mean temporal resolution of the  $^{10}\text{Be}$  record is about 5 years for this time interval.

[20] For the climatically relatively stable Holocene there are good reasons to assume that the climate system effects on the  $^{10}\text{Be}$  concentration measured in the GRIP ice core are small enough to be neglected in a first-order approximation. Probably the strongest argument comes from the comparison with the cosmogenic radionuclide  $^{14}\text{C}$  whose production is influenced by the same modulation processes but which, once produced, shows a completely different geochemical behavior as it participates in the global carbon cycle. Despite these fundamentally different geochemical systems, both records show a high degree of similarity throughout the Holocene. This strongly points to production as the dominant cause of variability [Muscheler et al.,

2004]. Further investigation is needed to analyze the cause for a slight discrepancy in the long-term trend (in the order of 10%), which can be due to system effects on both radionuclide records, like local changes in the atmospheric mixing, transport, or deposition and/or changes in the carbon cycle, respectively. However, within the relatively big uncertainties, the long-term changes of the GRIP  $^{10}\text{Be}$  data can be completely explained by changes in the geomagnetic field intensity indicating neither solar activity nor transport changes on timescales longer than 3000 years [Muscheler et al., 2005a]. The differences between  $^{14}\text{C}$  and independent geomagnetic field reconstructions could be explained by changes in the carbon cycle affecting the atmospheric  $^{14}\text{C}$  record [Muscheler et al., 2005a] and, in this case, making it problematic to use radiocarbon records to reconstruct long-term changes in solar activity.

[21] In Greenland,  $^{10}\text{Be}$  is mainly removed from the atmosphere by wet deposition. Changes in the precipitation rate as observed during glacial times can cause considerable changes in the  $^{10}\text{Be}$  concentration that are not related to the production rate [Wagner et al., 2000]. Calculating the  $^{10}\text{Be}$  flux as the product of  $^{10}\text{Be}$  concentration, accumulation rate, and density takes the variable accumulation conditions into account. However, during the Holocene the accumulation rate is relatively constant compared to the production rate variations leading to a  $^{10}\text{Be}$  flux that agrees well with the  $^{10}\text{Be}$  concentration. Stable climatic conditions can further be deduced from the fact that there are no indications for strong changes in the precipitation source for central Greenland during the Holocene [Johnsen et al., 1989; Mayewski et al., 1997]. This finding also holds information about the atmospheric pathway of  $^{10}\text{Be}$ , which, attached to aerosols, is also transported by the air masses. On the basis of the relatively stable transport and depositional processes at the coring site, we assume that in a first approximation, the  $^{10}\text{Be}$  flux, as well as the  $^{10}\text{Be}$  concentration, can be considered as a good estimate of the production signal free of climatic effects during the Holocene.

#### 5. Reconstruction of Solar Variability

##### 5.1. Method

[22] Our method to reconstruct the past solar activity relies on the well-established relationship between the geomagnetic field intensity, the  $^{10}\text{Be}$  production rate and the solar modulation function  $\Phi$  [Masarik and Beer, 1999], as illustrated in Figure 3. Using this relationship, the past solar activity expressed by  $\Phi$  can be derived from the  $^{10}\text{Be}$  production rate, provided that the past geomagnetic field intensity is known.

[23] Information on the past geomagnetic field intensity is obtained from archaeomagnetic investigations throughout the Holocene by Yang et al. [2000] (Figure 4a). They averaged measurements of the geomagnetic field strength from different regions of the Earth (mainly Europe and Asia) to assess the global geomagnetic dipole field. In order to level out short-term variations, which were assumed to be changes of the nondipole field [Yang et al., 2000], these data were averaged over 500 years (from 0 to 2000 years BC) and 1000 years (from 2000 years to 10,000 years BC) [Yang et al., 2000]. We did a spline interpolation of the originally stepwise paleomagnetic field record through the average

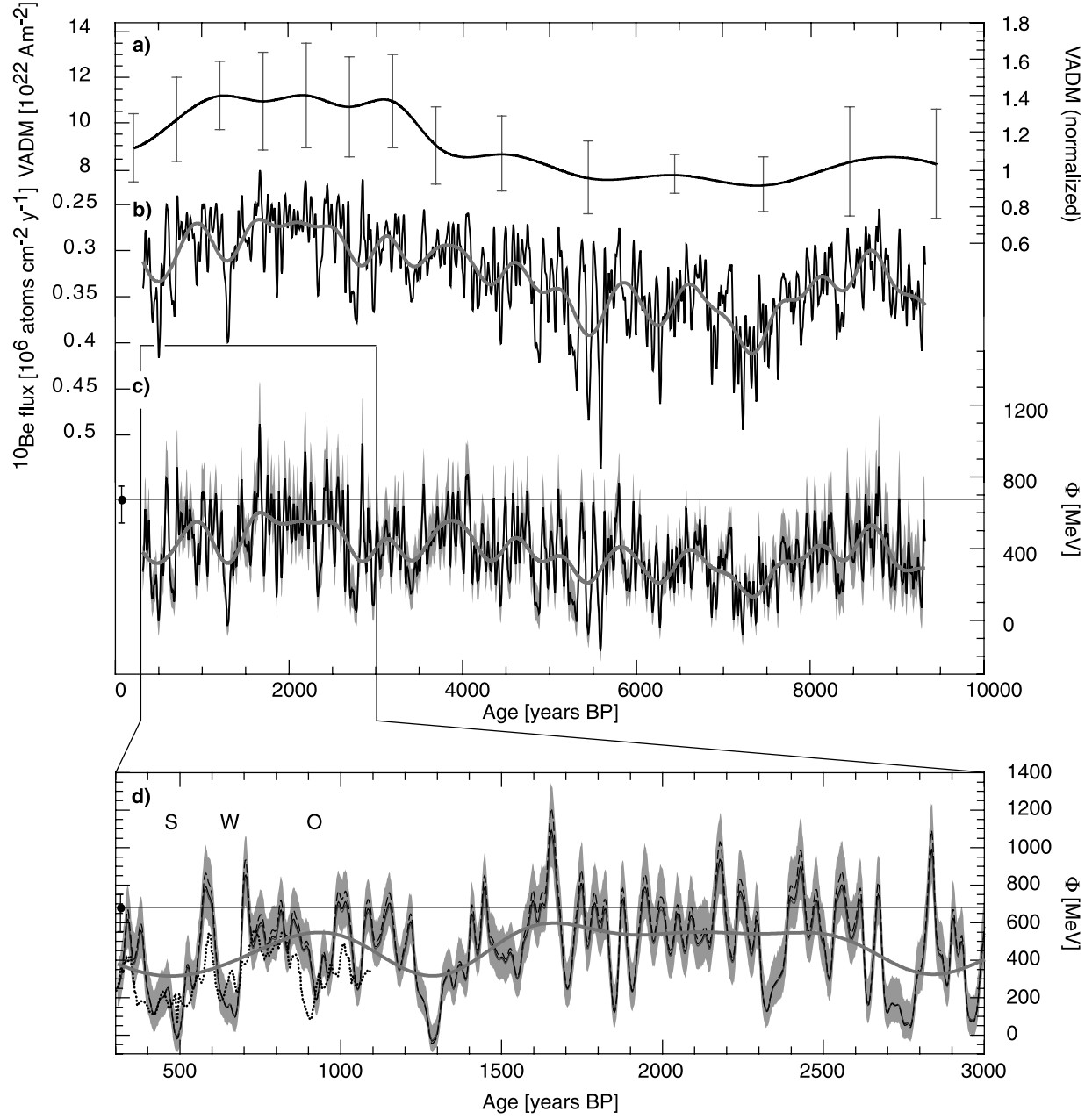


**Figure 4.** Reconstruction of the solar activity  $\Phi$  based on  $^{10}\text{Be}$ . (a) The geomagnetic dipole moment VADM (virtual axial dipole moment) with the standard deviation after Yang *et al.* [2000]. The right scale is in units relative to today. (b)  $^{10}\text{Be}$  flux extracted from the GRIP ice core, 61-point (data at identical 2-year intervals) binomial filtered (black curve). To visualize changes on longer periods a low pass filter (cutoff frequency =  $1/500 \text{ years}^{-1}$ ) (light gray curve) is applied to the original  $\Phi$  record. The data are plotted on an inverse scale. (c) Solar modulation function  $\Phi$  as derived from the binomial filtered  $^{10}\text{Be}$  (black curve) and after additionally low pass filtered (cutoff frequency =  $1/500 \text{ years}^{-1}$ ) (gray curve). The gray band shows the  $1\sigma$  errors. The isolated point close to the left y-axis and the black line, respectively, represent the mean  $\Phi$  value ( $\sim 680 \text{ MeV}$ ) of the four different  $\Phi$  reconstructions shown in Figure 2 (see caption there and text for detail) over the time interval 1958–1990 with an indication of the range of differences in the mean value of these reconstructions. Note that the point is not at the right position on the timescale. (d) A close-up view of Figure 4c with two additional  $\Phi$  reconstructions considering alternative assumptions of the  $^{10}\text{Be}$  flux showing a rather local or global signal: the gray curve (which is almost identical to the black curve over much of the record) represents a more local signal than the black curve and the dashed black curve represents a global production signal (see text for detail). The dotted black curve shows the  $\Phi$  record of McCracken *et al.* [2004] covering the past 1100 years for comparison. This close-up view further displays the recent grand solar minima in more detail, with S = Spörer Minimum (1415–1535 AD), W = Wolf Minimum (1280–1340 AD), and O = Oort Minimum (1010–1050 AD).

geomagnetic field values (Figure 4a) and numerically resampled it to get the same time resolution as in the case of  $^{10}\text{Be}$ , see below.

[24] Past  $^{10}\text{Be}$  production rates are derived from the measured  $^{10}\text{Be}$  concentrations in the GRIP ice core. In a first step, the  $^{10}\text{Be}$  concentration was converted into fluxes using the accumulation rate of *Johnsen et al.* [1995]. The data set was numerically resampled by linear interpolation to a constant time interval of 2 years. The short-term scatter in the  $^{10}\text{Be}$  record, probably caused by short-term changes in meteorological conditions, was removed by applying a 61-point binomial filter. Its effect is similar to a 25-year running mean (Figure 4b). Thereby, both the poorly resolved 11-year solar cycle and the weak 22-year magnetic Hale cycle are suppressed, but leaving changes on longer timescales, like the 88-year Gleissberg cycle [Gleissberg, 1965] or decades-long grand solar minima in the  $^{10}\text{Be}$  flux record (Figure 4b).

[25] The remaining changes in the  $^{10}\text{Be}$  flux are assumed to be related to variations in the atmospheric production rate. However, until now, no physical model is available to simulate accurately the atmospheric pathway of  $^{10}\text{Be}$  produced in the atmosphere to its deposition site.

[26] In previous publications, we assumed that the  $^{10}\text{Be}$  flux to Summit in Greenland reflects the globally averaged  $^{10}\text{Be}$  production rate. This rather simple assumption led to a very good agreement between the  $^{10}\text{Be}$ -based reconstructions of the geomagnetic field with independent geomagnetic field records on timescales longer than 3000 years [Muscheler et al., 2005a; Wagner et al., 2000]. However, owing to the rather short residence time of weeks in the troposphere [Raisbeck et al., 1981], an incomplete mixing of  $^{10}\text{Be}$  in the troposphere cannot be excluded and has to be considered for investigations of second-order effects. The polar  $^{10}\text{Be}$  production signal is distinctly solar modulated because of the weak or missing shielding effect of the geomagnetic field at high latitudes. Incomplete atmospheric mixing is expected to result in a larger contribution of polar produced  $^{10}\text{Be}$  in the polar  $^{10}\text{Be}$  deposition with an increased imprint of solar variations compared to a  $^{10}\text{Be}$  flux elsewhere on the globe. Consequently, without consideration of the prevailing mixing state of  $^{10}\text{Be}$  in the atmosphere, the variations in  $\Phi$  deduced from  $^{10}\text{Be}$  from GRIP ice core could possibly turn out to be too large. Different degrees of mixing of  $^{10}\text{Be}$  in the atmosphere and the effect on the reconstructed solar modulation will be discussed in section 6. Including a modification toward a slightly more “polar biased”  $^{10}\text{Be}$  signal improves the agreement with the record of the solar modulation function published by *McCracken et al.* [2004]. However, the relative contribution of the  $^{10}\text{Be}$  production in the stratosphere is higher than that of the troposphere [Masarik and Beer, 1999]. Therefore earlier paleogeomagnetic field records obtained from the  $^{10}\text{Be}$  data [Muscheler et al., 2005a; Wagner et al., 2000] are not compromised by this modification because the considered deviation of total mixing has a small impact on the geomagnetic field reconstruction.

[27] Because of the rather long residence time of about 1 year in the stratosphere compared to weeks in the troposphere [Raisbeck et al., 1981], we assume that the  $^{10}\text{Be}$  flux to Summit reflects the globally averaged  $^{10}\text{Be}$  production rate of the stratosphere but only the averaged

$^{10}\text{Be}$  production rate between  $40^\circ$  and  $90^\circ$  geographic latitudes of the troposphere. This assumption of no tropospheric contribution of produced  $^{10}\text{Be}$  from lower latitudes than  $40^\circ$  in the  $^{10}\text{Be}$  flux to Greenland is based on the pattern of the general circulation of the atmosphere. The effective descending air current from the Hadley Cell located at around  $30^\circ$  is assumed to remove the produced  $^{10}\text{Be}$  prior to its transport toward higher geographic latitudes. These assumptions are corroborated by the finding that the source of water vapor for central Greenland is situated in midlatitudes and did not change over the past 10,000 years [Johnsen et al., 1989; Mayewski et al., 1997]. However, as long as the exact atmospheric processes are not known, the mixing degree of  $^{10}\text{Be}$  in the atmosphere cannot be identified with certainty.

[28] Assuming this pattern of atmospheric mixing of  $^{10}\text{Be}$ , we need an additional free parameter in our model to link the  $^{10}\text{Be}$  flux into the Greenland ice shield to the  $^{10}\text{Be}$  production rate. Unfortunately, for reasons related to the drilling technique, there is no temporal overlap of the GRIP  $^{10}\text{Be}$  record with present  $\Phi$  values reconstructed from neutron monitor data. Therefore we selected the 795 year long period for which our  $^{10}\text{Be}$  record overlaps with the  $\Phi$  record derived from an Antarctic ice core [McCracken et al., 2004]. Given the geomagnetic field intensity data, we applied iteratively the relationship of *Masarik and Beer* [1999] (Figure 3) with the  $^{10}\text{Be}$  flux tuned to fit best the resultant  $\Phi$  record on this overlap part with the corresponding mean  $\Phi$  value in the  $\Phi$  record of *McCracken et al.* [2004]. This mean  $\Phi$  value is  $\sim 310$  MeV. However, this value was derived based on the local interstellar spectrum of *Webber and Lockwood* [2001] (dashed curve in Figure 1). To correct for the difference between this spectrum and the one we use, 90 MeV (determined empirically) have to be added leading to a mean value for the overlap time of  $\sim 400$  MeV.

[29] This normalization procedure provides an indication of the relationship between the  $^{10}\text{Be}$  flux to the GRIP ice core location and the  $^{10}\text{Be}$  production rate during this 795 years long period and, consequently, of the then atmospheric processes influencing the produced  $^{10}\text{Be}$ . Both the atmospheric mixing condition and the relationship between  $^{10}\text{Be}$  flux and  $^{10}\text{Be}$  production rate were assumed to be constant throughout the entire Holocene, although changing system processes cannot totally be ruled out. However, there are reasonable arguments that support the assumption of stable mixing, transport, and deposition processes during the Holocene (discussed in section 4). Implications of these system uncertainties on the  $\Phi$  record are discussed in sections 7 and 8.

## 5.2. Determination of the Error

[30] To calculate the error of the  $\Phi$  reconstruction, we ran 1000 Monte Carlo simulations taking into account the uncertainties both in the involved  $^{10}\text{Be}$  data and the geomagnetic field intensity data. The uncertainty of the filtered  $^{10}\text{Be}$  data is estimated to be 5%, which is the mean error of the accelerator mass spectrometry (AMS) analyses, rounded up to include potential sample preparation errors. The error of the paleomagnetic field strengths is the standard deviation specified by *Yang et al.* [2000]. Each Monte Carlo simulation involves  $^{10}\text{Be}$  and geomagnetic

field values randomly selected within their uncertainties, assuming Gaussian uncertainty distributions. It is important to note that this procedure leads to an upper limit of the absolute errors. The reason is that by selecting for each individual  $^{10}\text{Be}$  data point an independent geomagnetic field intensity based on the mean error of intervals of 500–1000 years (Figure 4a), we neglect the fact that the geomagnetic dipole field can only change on centennial to millennial timescales. Therefore the  $\Phi$  errors obtained in this way are maximal absolute  $1\sigma$  errors. They range from  $\sim 60$  MeV to  $\sim 290$  MeV with a mean of  $\sim 140$  MeV for the analyzed period. Taking into account the inertia of the geomagnetic field, the uncertainty of the relative short-term  $\Phi$  changes is reduced to a range from  $\sim 40$  MeV to  $\sim 150$  MeV with a mean of  $\sim 80$  MeV. This uncertainty resulting from the error of the  $^{10}\text{Be}$  data is thus comparable with the different neutron monitor-based reconstructions of  $\Phi$  for the past 50 years using different models (see Figure 2). Owing to the nonlinearity of the relationship between production rate, geomagnetic dipole moment, and  $\Phi$ , the error transformation is also nonlinear. As the  $^{10}\text{Be}$  production rate is inversely proportional to  $\Phi$ , high  $\Phi$  values are highly sensitive to errors in low  $^{10}\text{Be}$  values. Low prevailing geomagnetic field intensity further amplifies this transformation effect of the  $^{10}\text{Be}$  uncertainty on the calculated  $\Phi$ . The error of the geomagnetic dipole moment itself has a stronger influence on the  $\Phi$  calculation in the low field range than in the high field range.

## 6. Results

[31] The record of solar activity in terms of the solar modulation function  $\Phi$  for about the last 9300 years, reconstructed from the geomagnetic field intensity of Yang *et al.* [2000] (Figure 4a) and the GRIP  $^{10}\text{Be}$  flux (Figure 4b), is displayed in Figure 4c. The gray error band comprehends uncertainties resulting from errors of the  $^{10}\text{Be}$  data and of the geomagnetic field intensities. Since the geomagnetic dipole field varies only very slowly (on centennial to millennium timescales) the error of the relative changes of  $\Phi$  on short timescales (decadal to centennial) is not affected by the absolute uncertainty of the geomagnetic field intensities and therefore much smaller than shown by this error band. Although the  $\Phi$  record is calculated based on the filtered  $^{10}\text{Be}$  flux in which periods shorter than about 50 years are increasingly suppressed (with periods shorter than about 22 years being almost completely suppressed) (black curve), the  $\Phi$  record is characterized by a high and persistent variability throughout the Holocene. It clearly reproduces the well-known grand solar minima Spörer (1415–1535 AD), Wolf (1280–1340 AD), and Oort (1010–1050 AD), as it is highlighted in a close-up view of the  $\Phi$  record covering the past 3000 years (Figure 4d).

[32] Owing to the difference in the long-term trend between the  $^{10}\text{Be}$  and  $^{14}\text{C}$  record, statements on absolute  $\Phi$  values and on long-term changes have to be made with caution (see sections 7 and 8). In addition, the absolute values depend on the normalization, for which we rely on the mean  $\Phi$  value in McCracken *et al.*'s [2004]  $\Phi$  record for the overlap time with our  $\Phi$  record. Nevertheless, this normalization looks reasonable in the sense that it does

not reveal systematically negative  $\Phi$  values nor extremely high  $\Phi$  values exceeding significantly the recent rather high  $\Phi$  estimates (see Figure 2).

[33] The timing and the relative amplitude of short-term fluctuations of  $\Phi$ , however, are much more certain since the production rate dependency on the geomagnetic field intensity and the solar modulation are well known [Masarik and Beer, 1999]. The relative amplitude only depends slightly on the normalization due to the nonlinearity of those dependencies. The uncertainty of the relative amplitude due to the unknown mixing degree of  $^{10}\text{Be}$  in the atmosphere is considerably reduced as in this case the latter can be constricted quite well (see below). Therefore the strength of the records is the relative amplitude of solar modulation changes during the Holocene.

[34] To visualize the amplitude dependency of the  $\Phi$  record on the mixing assumption for the  $^{10}\text{Be}$  flux to Summit, two additional records were calculated considering alternative degrees of mixing (Figure 4d). One record is based on the assumption that the  $^{10}\text{Be}$  flux reflects the globally averaged production rate and the other one that the  $^{10}\text{Be}$  flux reflects the globally averaged stratospheric production rate but only the averaged tropospheric production rate within  $60^\circ$  and  $90^\circ$  geographic latitudes. We consider the latter as rather unlikely because of the midlatitude source of water vapor for Greenland [Johnsen *et al.*, 1989; Mayewski *et al.*, 1997]. The smaller the degree of atmospheric mixing of  $^{10}\text{Be}$ , the smaller the amplitude of the resulting  $\Phi$  record. However, as the relative  $^{10}\text{Be}$  production in the globally mixed stratosphere is much higher than in the restricted troposphere, the effect of these different assumptions is small. To evaluate our mixing approaches, we compare our reconstruction with the solar modulation record for the past 1100 years (22-year averages) estimated by McCracken *et al.* [2004] (Figure 4d). The assumption that  $^{10}\text{Be}$  does not reflect a globally mixed troposphere improves the agreement with McCracken *et al.* [2004]. However, even the assumption of a rather local  $^{10}\text{Be}$  signal at Summit (tropospheric component restricted to  $60^\circ$  to  $90^\circ$  geographic latitudes) results in a  $\Phi$  record with a larger amplitude than that of McCracken *et al.*'s [2004]  $\Phi$  record. It is important to note that the amplitude of McCracken *et al.*'s [2004]  $\Phi$  record itself depends on the assumption of an incomplete mixing of the used  $^{10}\text{Be}$  from the South Pole record, which they corrected for by involving an atmospheric mixing model (M3) [McCracken, 2004]. An above-average contribution of the high latitudes to the  $^{10}\text{Be}$  signal is concordant with results obtained by Steig *et al.* [1996] and Bard *et al.* [1997], who compared the amplitude of solar modulation of  $^{10}\text{Be}$  with that of cosmic rays and  $^{14}\text{C}$ , respectively. However, these investigations are restricted to Antarctica and probably not transferable to other regions. Because Greenland's precipitation source lies in midlatitudes we consider the mixing model (M3) used by McCracken *et al.* [2004] to be too restrictive for the GRIP  $^{10}\text{Be}$  data. New calculations of the  $^{14}\text{C}$  production rate and the resulting solar modulation changes for the last millennium also indicate a higher variability in solar activity than the one given by McCracken *et al.* [2004; Muscheler *et al.*, 2006]. Owing to the nonlinear relationship between  $\Phi$  and  $^{10}\text{Be}$  production rate (see Figure 3), high  $\Phi$  values are more sensitive to the considered mixing degree of  $^{10}\text{Be}$  in the

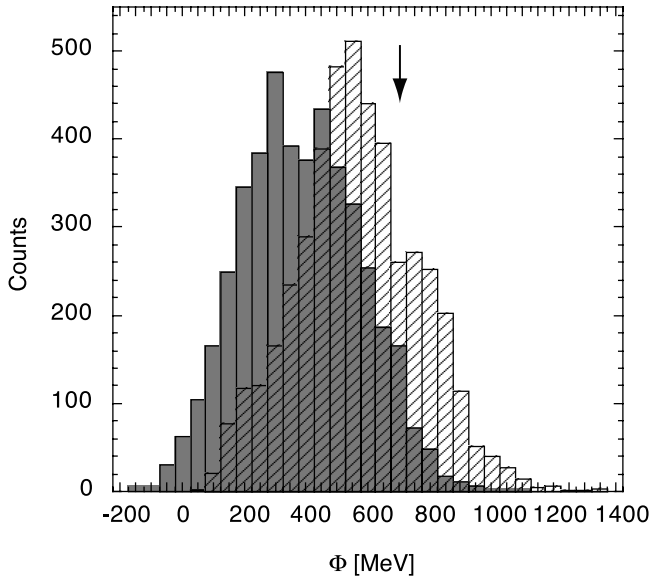


**Figure 5.** The distribution of  $\Phi$  values during the Holocene in a histogram with a class width of 50 MeV. Note that the absolute  $\Phi$  values are dependent on the required normalization and on the long-term trend of the  $\Phi$  record, which is still uncertain. The histogram in gray shows the counts of  $\Phi$  values of the presented record based on the 61-point (at identical 2-year intervals) binomial filtered  $^{10}\text{Be}$  flux.  $\Phi$  varied in the range of 0 MeV to 1070 MeV, with most values around 300 MeV. The mean  $\Phi$  value of the record is  $\sim 370$  MeV, the median  $\sim 360$  MeV, and the standard deviation  $\sim 190$  MeV. The hatched histogram results from the reconstruction of  $\Phi_{14\text{C}}$  using the 61-point (at identical 2-year intervals) binomial filtered  $^{14}\text{C}$  production rate of *Stuiver and Braziunas* [1988] instead of  $^{10}\text{Be}$ . This  $\Phi_{14\text{C}}$  record ranged between 50 MeV and 1340 MeV during the 9000 years correspondent to the  $^{10}\text{Be}$ -based  $\Phi$  record. Most values are around 550 MeV. The mean value of the  $\Phi_{14\text{C}}$  record is  $\sim 550$  MeV, the median  $\sim 540$  MeV, and the standard deviation  $\sim 200$  MeV. The arrow indicates the position of the average modulation function of the past 50 years (710 MeV) as derived by *Masarik and Beer* [1999].

atmosphere than low  $\Phi$  values. Therefore the larger amplitude in our curve compared to the amplitude in the curve of *McCracken et al.* [2004] is mainly expressed in higher solar maxima than those of *McCracken et al.*'s [2004] record.

[35] The  $\Phi$  record shows various periods of highly variable solar activity, especially pronounced around 700, 1850, 2650, and 5950 years BP when the filtered  $\Phi$  values shifted up to 470 MeV within  $\sim 20$  years. The most stable periods are centered around 1500, 4850, 5250, and 8350 years BP, showing a smaller variability in comparison to the 50 years long present neutron monitor era. Spectral analysis distinctly reveals the known solar cycles at periodicities of 88 years (Gleissberg cycle) and 208 years (De Vries cycle).

[36] The values of our  $\Phi$  record varied generally in the range of 0 MeV to 1070 MeV. Our record shows some values which lie below 0 MeV which cannot represent a real state of the Sun (0 MeV is defined as no solar modulation). However, within the  $1\sigma$  error (see section 5.2) all negative

values of  $\Phi$  are in agreement with  $\Phi \geq 0$  MeV, except for the negative peaks around 5670 and 7210 years BP. The distribution of the filtered  $\Phi$  values in this solar activity record shows that  $\Phi$  values around 300 MeV are most frequent. The arithmetic mean of the record is  $\sim 370$  MeV (see gray histogram in Figure 5), which is lower than the mean  $\Phi$  value of 550 MeV over a few millions of years proposed by *Masarik and Reedy* [1994].

[37] Obvious are several modes of temporary reduced solar activity throughout the Holocene analogous to the historical grand solar minima confirming clearly the larger variability potential of the Sun on longer timescales than observed during the  $\sim 50$  years long period of neutron monitors. The weakest historical grand solar minimum reproduced in our  $\Phi$  record is the Oort Minimum. Overall, the Sun's activity was for about 35% of the investigated time in a status comparable to a grand solar minimum as the Oort Minimum with a mean of  $\sim 280$  MeV. Between 7100 and 7650 years BP the Sun's activity was constantly that low, interrupted only once by 20 years. Grand solar minima comparable to the most pronounced Spörer Minimum in our  $\Phi$  record (mean ( $\sim 150$  MeV), minimum ( $\sim 0$  MeV), and maximum ( $\sim 340$  MeV)), however, occurred for about 8% of the investigated time (e.g., extending over 300 years around 7250 years BP). On the other hand, there were several time periods as long or longer than the neutron monitor era with similar or higher solar modulation compared to the last 50 years (around 1650 and 2400 years BP, with the highest mean  $\Phi$  value over 50 years of  $\sim 860$  MeV around 1650 years BP). These periods of high solar activity extended over about 1% of the investigated time. Taking into consideration the maximal uncertainty of our  $\Phi$  reconstruction, that is, the lower and upper limit of the error band, we estimate that such periods of high solar activity covered 0% (lower limit of the error band) and 11% (upper limit of the error band), respectively, of the investigated 9000 years. In all, irrespective of the duration, the filtered  $\Phi$  values were for about 7% (1% and 18% considering the lower and upper limit of the  $1\sigma$  error band, respectively) of the investigated time higher than during the neutron monitor era. The present neutron monitor era with a mean  $\Phi$  value of about 680 MeV is among the periods with the highest level of solar activity for the past 9300 years. However, our  $\Phi$  record clearly indicates that the present Sun's high activity period is not so unusual regarding the entire Holocene.

## 7. Assessment of the Record's Uncertainties Concerning its Long-Term Trend

[38] The reconstructed  $\Phi$  record displays a long-term trend (Figure 4c). Inferring a varying solar activity on such long timescales is not possible as long as the mentioned uncertainties considering possible system effects of the  $^{10}\text{Be}$  record exist and geomagnetic field reconstructions during the Holocene exhibit such large errors. Within the uncertainties, the long-term changes in  $^{10}\text{Be}$  can be completely explained by the changes in the geomagnetic dipole field [*Muscheler et al.*, 2005a; *Wagner et al.*, 2000]. Taking into account the calculated errors of the  $\Phi$  reconstruction, the long-term trend in  $\Phi$  in fact turns out not to be significant, indicating that possible system effects on the  $^{10}\text{Be}$  flux would be small. Therefore the observed long-term trend in

the presented  $\Phi$  record is most likely caused by an incomplete elimination of the geomagnetic field influence on the  $^{10}\text{Be}$  flux and/or a slight long-term change in the climate system. However, long-term changes in solar activity cannot be excluded either.

[39] The analysis of additional  $^{10}\text{Be}$  records from other ice cores (e.g., Dronning Maud Land, Antarctica) as well as the modeling of the atmospheric pathway of  $^{10}\text{Be}$  after its production until its deposition, both works in progress, will contribute to clarify the source of the long-term trend by identifying local climatic influences on the  $^{10}\text{Be}$  records in more detail. Furthermore, improved geomagnetic field records are required to eliminate the geomagnetic field effect on the  $^{10}\text{Be}$  production rate with more certainty, especially as the geomagnetic field record of Yang *et al.* [2000] is possibly biased by the globally nonuniform distribution of the measured samples (located mostly in Europe and Asia). New reconstructions of the geomagnetic dipole field [Korte and Constable, 2005] generally show lower values and a different long-term trend than Yang *et al.* [2000] which is in better agreement with the long-term trend of the GRIP  $^{10}\text{Be}$  flux. Accordingly, a  $\Phi$  reconstruction using this geomagnetic field record will result in a different, smaller, long-term trend.

[40] The uncertainty of the long-term trend of the radionuclide record is not included in the assessed  $1\sigma$  error, as the latter considers the error of the  $^{10}\text{Be}$  data regarding its measurement but not possible system effects. However, this uncertainty has no impact on the determination of the short-term changes in  $\Phi$  apart from the effect due to the nonlinearity of the relationship between  $\Phi$  and  $^{10}\text{Be}$ . However, it has to be considered when comparing absolute values of this  $\Phi$  record throughout the Holocene.

## 8. Evaluation and Discussion of the Long-Term Trend in the $\Phi$ Record

[41] For a critical evaluation of the observed long-term trend of  $\Phi$ , we alternatively calculated  $\Phi$  using the  $^{14}\text{C}$  production rate from Stuiver and Braziunas [1988] with the production rate calculations for  $^{14}\text{C}$  from Masarik and Beer [1999]. The two radionuclide records are in good agreement considering their short-term variations but show discrepancies in their long-term trend presumably related to changed long-term system effects in either cosmogenic radionuclide record. Thus a comparison between the respective  $\Phi$  records allows a first quantitative assessment of the impact of these system uncertainties on the long-term trend of the presented  $\Phi$  record.

[42] The  $^{14}\text{C}$  production rate is corrected for the carbon cycle effect on the atmospheric  $^{14}\text{C}$  concentration by a carbon cycle model [Stuiver and Braziunas, 1988]. The record of the  $^{14}\text{C}$  production rate covers the entire Holocene based on a  $\Delta^{14}\text{C}$  record with a time resolution of 10 years. To account for the  $^{12}\text{C}$  accumulation in the atmosphere due to the combustion of fossil fuel since the industrialization (Suess [1953] effect), we did not use the last 150 years of the  $^{12}\text{C}$  production rate record of Stuiver and Braziunas [1988]. We filtered the data in the same way as the  $^{10}\text{Be}$  flux (61-point binomial filter, with data previously linearly interpolated at identical 2-year intervals). Owing to the atmospheric residence time of 4–5 years,  $^{14}\text{C}$  is assumed

to be well mixed within the atmosphere. Using the known dependency of the global  $^{14}\text{C}$  production rate on  $\Phi$  and the geomagnetic field intensity [Masarik and Beer, 1999] along with the geomagnetic field intensity record of Yang *et al.* [2000], the corresponding solar modulation function  $\Phi$  can be calculated. According to the  $^{10}\text{Be}$ -based  $\Phi$  record, the  $^{14}\text{C}$ -based  $\Phi$  record was normalized in order to obtain an average  $\Phi$  value consistent with McCracken *et al.*'s [2004]  $\Phi$  record (see section 5.1).

[43] Figure 6 shows the record of the solar modulation function  $\Phi$  resultant from the filtered global  $^{14}\text{C}$  production rate for the past 11,450 years. This  $\Phi$  record is indicated in the following as  $\Phi_{14\text{C}}$ , whereas  $\Phi$  without index refers to the  $^{10}\text{Be}$ -based  $\Phi$  record. Like the  $\Phi$  record, this  $\Phi_{14\text{C}}$  record reveals periods with a highly variable solar activity alternating with much more stable periods. High variability characterizes especially the times at 6000, 8100, 8850, and 9150 years BP with a shift of the filtered  $\Phi_{14\text{C}}$  values of up to 490 MeV within  $\sim$ 20 years. The most stable periods were around 3000, 3900, 5900, and 7000 years BP, showing a smaller variability in comparison with the present neutron monitor era.

[44] As expected from the involved radionuclide data, the comparison of the  $\Phi_{14\text{C}}$  record with the  $\Phi$  record reveals somewhat different long-term trends of the two records. Apart from a potential incomplete elimination of the geomagnetic field effect as a result of the large geomagnetic field record uncertainty, the long-term trend of the  $\Phi_{14\text{C}}$  record can be most probably attributed to changing system effects in the  $^{14}\text{C}$  record, possibly due to carbon cycle model uncertainties [Muscheler *et al.*, 2005a]. However, changes in the  $^{10}\text{Be}$  record or both records cannot be excluded. Owing to the same normalization of both  $\Phi$  records with McCracken *et al.*'s [2004]  $\Phi$  record in their overlap time period, the  $\Phi_{14\text{C}}$  record displays systematically higher values (on average  $\sim$ 250 MeV) in the early and middle Holocene than the  $\Phi$  record (Figure 6).

[45] As a result of the uncertainty of the long-term trend and the normalization, the absolute  $\Phi_{14\text{C}}$  values are not as reliable as the relative amplitude of short-term changes of  $\Phi_{14\text{C}}$ . The presented filtered  $\Phi_{14\text{C}}$  record extended over the range 50–1810 MeV with a mean value of  $\sim$ 610 MeV. For the following discussion we consider only the 9000 years corresponding to the  $^{10}\text{Be}$ -based  $\Phi$  record in which the  $\Phi_{14\text{C}}$  values varied between 50 and 1340 MeV with a mean value of  $\sim$ 550 MeV (and where carbon cycle model errors due to uncertain starting condition are of minor importance [Muscheler *et al.*, 2005a]). Figure 5 shows the distribution of the filtered  $\Phi_{14\text{C}}$  (hatched histogram) with most values being around 550 MeV and only a few values over 1100 MeV. The filtered  $\Phi_{14\text{C}}$  values of our reconstruction indicate for about 4% of the 9000 years a solar activity status at least as low as the Oort Minimum with a mean of  $\sim$ 190 MeV. These periods were all centered in the late Holocene. For the Spörer Minimum (mean ( $\sim$ 150 MeV), minimum ( $\sim$ 80 MeV), and maximum ( $\sim$ 240 MeV)) no counterpart was found in our  $\Phi_{14\text{C}}$  record, and therefore it could be considered as unique in the Holocene if the long-term trend indicated by  $^{14}\text{C}$  indeed would be correct. For about 27% of the investigated time the  $\Phi_{14\text{C}}$  values were higher than during the 50 years long neutron monitor period. Especially in the early and middle Holocene were

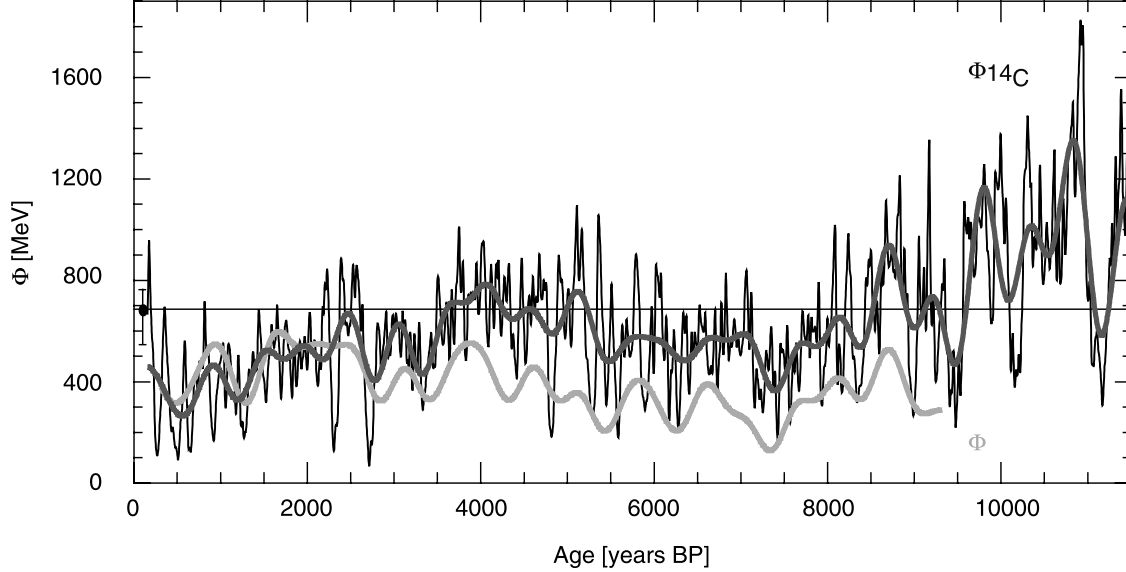


**Figure 6.** Reconstructed solar activity record in terms of the solar modulation function  $\Phi$  based on the  $^{14}\text{C}$  production rate of *Stuiver and Braziunas* [1988] and the geomagnetic field record of *Yang et al.* [2000] for the past 11,450 years. The black curve shows  $\Phi_{14\text{C}}$  resultant from the 61-point (at identical 2-year intervals) binomial filtered  $^{14}\text{C}$  production rate. A low pass filter (cutoff frequency =  $1/500 \text{ years}^{-1}$ ) (gray curve) is applied to visualize changes on longer time scales. The isolated point on the left hand side and the black line, respectively, mark the mean  $\Phi$  value during the neutron monitor era ( $\sim 680 \text{ MeV}$ ) including the range of the differences of these reconstructions (see Figure 2 and text for detail). The light gray curve displays the low pass filtered  $^{10}\text{Be}$ -based  $\Phi$  record from Figure 4c for comparison.

many periods lasting as long or longer than the neutron monitor era with similar or higher solar modulation, that is 21% of the 9000 years. There was one period around 8800 years BP displaying even a 320-year average  $\Phi_{14\text{C}}$  value of  $\sim 870 \text{ MeV}$ . These calculations yield the same result as the  $^{10}\text{Be}$ -based reconstruction, i.e., that today's solar activity is not that exceptional.

[46] The comparison of the two  $\Phi$  records gives a good impression of the uncertainty range in the  $\Phi$  record due to the uncertain long-term trend in the radionuclide records, as, most probably, the true  $\Phi$  values lie somewhere in between the two  $\Phi$  records. It shows that, e.g., changes in the  $^{10}\text{Be}$  flux in the order of only 10% in the early and middle Holocene due to possible long-term changes in the atmospheric transport processes or in the precipitation rate would be sufficient to remove the discrepancy between the two  $\Phi^{14\text{C}}$  records. Since the uncertainties of the available data are in this order of magnitude, we cannot pinpoint where the causes for these differences between the two radionuclide records lie. A long-term difference of only 10% justifies our previous general assumption of a constant  $^{10}\text{Be}$  transport and deposition at Summit during the Holocene and that the changes in the  $^{10}\text{Be}$  flux are dominated by variations in the  $^{10}\text{Be}$  production rate.

[47] Concerning their short-term structures, the two  $\Phi$  records agree generally very well what provides high confidence in the short-term  $\Phi$  reconstruction. To illustrate this similarity, both  $\Phi$  records were high pass filtered (cutoff frequency  $1/2000 \text{ years}^{-1}$ ) and displayed together in Figure 7. On closer examination, however, small differences in the amplitude between the two reconstructions reveal temporal changes in the  $^{10}\text{Be}$  transport and deposi-

tion at Summit during the Holocene and/or a temporary incorrect  $^{14}\text{C}$  production rate calculation due to changes in the carbon cycle. Except in the early Holocene, the amplitude of the  $\Phi$  record is generally slightly larger than that of the  $\Phi_{14\text{C}}$  record. Leads and lags in the  $\Phi$  record relative to the  $\Phi_{14\text{C}}$  record are most probably the result of uncertainties in the ss09 timescale of the GRIP ice core.

[48] Using two different radionuclide records thus enables a more precise assessment of the uncertainties of the  $\Phi$  reconstruction. Apart from the known uncertainty of the involved geomagnetic field record, the reconstruction with the two cosmogenic radionuclide records uncovers disregarded system effects on long timescales of at least one radionuclide record. Up to now, it is not possible to conclude if either of the radionuclide records is correct and thus the long-term trend of the respective  $\Phi$  record caused only by an imperfect elimination of the geomagnetic field influence. With an improved geomagnetic field record, the possible uncertainty of the used radionuclide record will be a deciding factor for the interpretation of the long-term changes in  $\Phi$ . Therefore detailed system investigations are required regarding both the atmospheric mixing, transport, and deposition processes of  $^{10}\text{Be}$  and possible carbon cycle changes concerning the atmospheric concentration of  $^{14}\text{C}$ .

[49] *Solanki et al.* [2004] reconstructed sunspot numbers for the past 11,450 years based on basically the same  $^{14}\text{C}$  record but concluded a current high solar activity level unprecedented in intensity as well as in duration for the last 8000 years. Unlike our  $\Phi$  reconstruction, they reconstructed a solar activity parameter (sunspots) related to the magnetic flux at the photosphere. This implicates an additional uncertainty because the used proxy data ( $^{14}\text{C}$ )

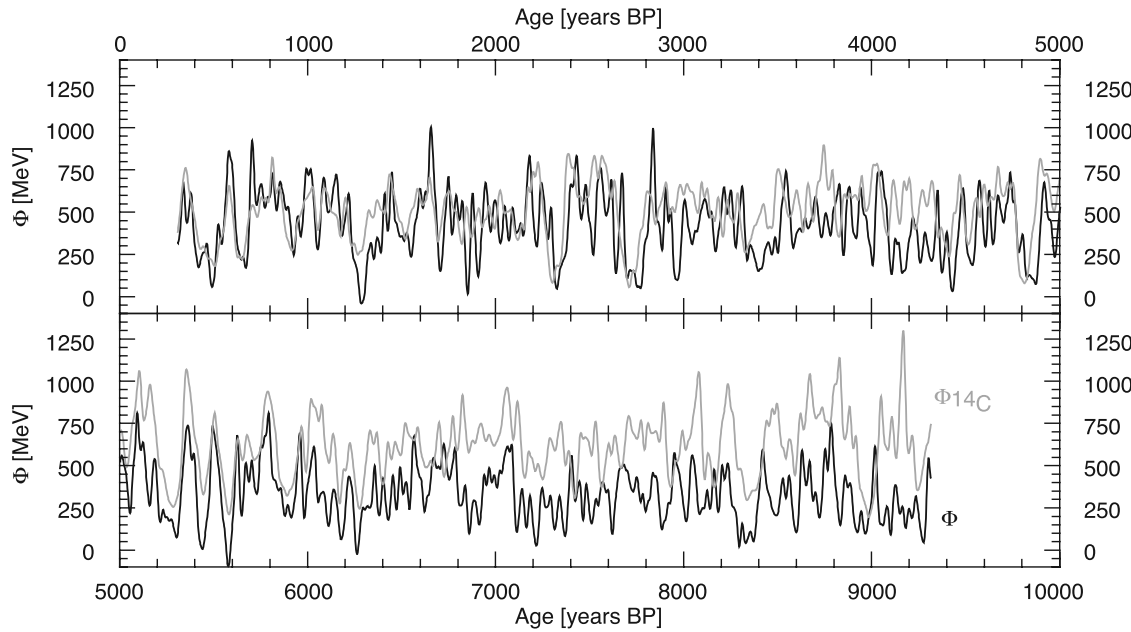


**Figure 7.** Comparison of  $\Phi$  reconstructed from  $^{10}\text{Be}$  (black curve) with  $\Phi$  reconstructed from the  $^{14}\text{C}$  production rate ( $\Phi_{^{14}\text{C}}$ , gray curve). Both  $\Phi$  records are high pass filtered (cutoff frequency  $1/2000 \text{ years}^{-1}$ ) to remove their different long-term trends.

are related to the open magnetic flux whose connection to the closed magnetic flux is only poorly understood. However, most important is that our  $\Phi$  reconstruction indicates that Solanki *et al.*'s [2004] main statement based on the long-term trend needs to be reconsidered since our analysis indicates that neither the  $^{10}\text{Be}$  nor the  $^{14}\text{C}$  record supports their conclusions.

## 9. Conclusions and Outlook

[50] Cosmogenic radionuclides like  $^{10}\text{Be}$  and  $^{14}\text{C}$  have a large potential to reconstruct past solar activity. Taking the past changes in geomagnetic dipole field intensity into account, a quantitative record of solar activity in terms of the solar modulation function  $\Phi$  has been calculated for the past 9300 years.

[51] The  $\Phi$  record is characterized by a high short-term variability of solar activity throughout the entire Holocene. The reconstructed solar activity record is a robust record regarding the relative amplitude and the occurrence of short-term (decadal to centennial) variations in  $\Phi$ , that is, the detection of periods of a high or low variability, or of periods of generally high or low solar activity levels and thus of grand solar minima. As far as the long-term trend is concerned there is a slight discrepancy between the reconstructions based on  $^{10}\text{Be}$  and  $^{14}\text{C}$ . Whether this discrepancy is mainly due to changes in the  $^{14}\text{C}$  or the  $^{10}\text{Be}$  system cannot yet be decided without further information.

[52] The  $\Phi$  record provides a quantitative parameter of solar activity with a long-term perspective in the field of solar and cosmic ray physics compared to the decadal and centennial long direct solar activity proxies and neutron monitor records of the past 50 years. Furthermore, this detailed record of  $\Phi$  has a large impact on the investigation of past solar forcing on Earth's climate as it provides a very promising basis for solar irradiance reconstructions.

[53] Comparing the solar activity of the last 50 years with the presented  $\Phi$  record, it is obvious that the recent neutron monitor records reflect a solar activity not representative regarding the average state of the Sun during the Holocene for two reasons. (1) The variability of  $\Phi$  during the neutron monitor period is much smaller than the average variability during the Holocene. (2) The level of solar activity over the past 50 years is indeed high. However, looking at the solar activity record for the entire Holocene, this high level of solar activity and its duration is rare but not outstanding. Both  $^{10}\text{Be}$  and  $^{14}\text{C}$  indicate that there were various periods of a similar length as the neutron monitor era where similar or higher  $\Phi$  conditions occurred. This is in contrast to the studies of Usoskin *et al.* [2003] and Solanki *et al.* [2004] who did not find comparable high solar activity periods for the past 1150 and 8000 years, respectively, and therefore claim that there has been an exceptionally active Sun since the 1940s.

[54] The accuracy of the absolute values of the presented  $\Phi$  record will significantly be enhanced by an improved geomagnetic field record. Further research is needed on  $^{10}\text{Be}$  records from other ice cores concerning variable system effects and on the  $^{14}\text{C}$  production rate calculation to better constrain the long-term trend of the reconstructed solar activity records.

[55] **Acknowledgments.** We would like to thank Irene Brunner from the EAWAG and Peter W. Kubik from the AMS facility at ETH in Zurich for sample preparation and taking care of the  $^{10}\text{Be}$  measurements, respectively. This work was supported by the Swiss National Science Foundation.

[56] Shadia Rifai Habbal would like to thank Claus Frohlich and two other referees for their help in evaluating this paper.

## References

- Baliunas, S., and R. Jastrow (1990), Evidence for long-term brightness changes of solar-type stars, *Nature*, 348, 520–523.

- Bard, E., G. M. Raisbeck, F. Yiou, and J. Jouzel (1997), Solar modulation of cosmogenic nuclide production over the last millennium: comparison between  $^{14}\text{C}$  and  $^{10}\text{Be}$  records, *Earth. Planet. Sci. Lett.*, **150**, 453–462.
- Bard, E., G. M. Raisbeck, F. Yiou, and J. Jouzel (2000), Solar irradiance during the last 1200 years based on cosmogenic nuclides, *Tellus, Ser. B*, **52**, 985–992.
- Baumgartner, S., J. Beer, M. Suter, B. Dittrich-Hannen, H.-A. Synal, P. W. Kubik, C. Hammer, and S. Johnsen (1997a), Chlorine 36 fallout in the Summit Greenland Ice Core Project ice core, *J. Geophys. Res.*, **102**, 26,659–26,662.
- Baumgartner, S., J. Beer, G. Wagner, P. W. Kubik, M. Suter, G. M. Raisbeck, and F. Yiou (1997b),  $^{10}\text{Be}$  and dust, *Nucl. Instrum. Methods Phys. Res., Sect. B*, **123**, 296–301.
- Beer, J. (2000a), Long-term indirect indices of solar variability, *Space Sci. Rev.*, **11**, 53–66.
- Beer, J. (2000b), Neutron monitor records in broader historical context, *Space Sci. Rev.*, **93**, 107–119.
- Beer, J., S. M. Tobias, and N. O. Weiss (1998), An active Sun throughout the Maunder minimum, *Solar Phys.*, **181**, 237–249.
- Bond, G., B. Kromer, J. Beer, R. Muscheler, M. N. Evans, W. Showers, S. Hoffmann, R. Lotti-Bond, I. Hajdas, and G. Bonani (2001), Persistent solar influence on North Atlantic climate during the Holocene, *Science*, **294**, 2130–2136.
- Bonino, G., G. Cini Castagnoli, D. Cane, C. Taricco, and N. Bhandari (2001), Solar modulation of the galactic cosmic ray spectra since the Maunder minimum, paper presented at ICRC 2001, Copernicus Gesellschaft 2001, Hamburg, Germany.
- Caballero-Lopez, R. A., and H. Moraal (2004), Limitations of the force field equation to describe cosmic ray modulation, *J. Geophys. Res.*, **109**, A01101, doi:10.1029/2003JA010098.
- Caballero-Lopez, R. A., H. Moraal, K. G. McCracken, and F. B. McDonald (2004), The heliospheric magnetic field from 850 to 2000 AD inferred from  $^{10}\text{Be}$  records, *J. Geophys. Res.*, **109**, A12102, doi:10.1029/2004JA010633.
- Cini Castagnoli, G., and D. Lal (1980), Solar modulation effects in terrestrial production of carbon-14, *Radiocarbon*, **22**, 133–158.
- Denton, G. H., and W. Karlén (1973), Holocene climatic variations - their pattern and possible cause, *Quat. Res.*, **3**, 155–205.
- Eddy, J. A. (1976), The Maunder Minimum, *Science*, **192**, 1189–1201.
- Finkel, R. C., and K. Nishizumi (1997), Beryllium-10 concentrations in the Greenland ice sheet project 2 ice core from 3–40 ka, *J. Geophys. Res.*, **102**, 26,699–26,706.
- Fleitmann, D., S. J. Burns, M. Mudelsee, U. Neff, J. Kramers, A. Mangini, and A. Matter (2003), Holocene forcing of the Indian Monsoon recorded in a stalagmite from Southern Oman, *Science*, **300**, 1737–1739.
- Fröhlich, C., and J. Lean (1998), The Sun's total irradiance: Cycles, trends and related climate change uncertainties since 1976, *Geophys. Res. Lett.*, **25**, 4377–4380.
- Fröhlich, C. (2006), Solar irradiance variability since 1978: Revision of the PMOD composite during solar cycle 21, *Space Sci. Rev.*, in press.
- Gleeson, L. J., and W. I. Axford (1968), Solar modulation of galactic cosmic rays, *Astrophys. J.*, **154**, 1011–1018.
- Gleissberg, W. (1965), The eighty-year solar cycle in auroral frequency numbers, *J. Br. Astron. Assoc.*, **75**, 227.
- Haigh, J. D. (1994), The role of stratospheric ozone in modulating the solar radiative forcing of climate, *Nature*, **370**, 544–546.
- Haigh, J. D. (1996), The Impact of solar variability on climate, *Science*, **272**, 981–984.
- Haigh, J. D. (1999), Modelling the impact of solar variability on climate, *J. Atmos. Sol. Terr. Phys.*, **61**, 63–72.
- Hall, J. C., and G. W. Lockwood (2004), The chromospheric activity and variability of cycling and flat activity solar-analog stars, *Astrophys. J.*, **614**, 942–946.
- Hodell, D. A., M. Brenner, J. H. Curtis, and T. Guilderson (2001), Solar forcing of drought frequency in the Maya lowlands, *Science*, **292**, 1367–1370.
- Hoyt, D. V., and K. H. Schatten (1998), Group sunspot numbers: a new solar activity reconstruction, *Solar Phys.*, **179**, 189–219.
- Johnsen, S. J., W. Dansgaard, and J. W. C. White (1989), The origin of Arctic precipitation under present and glacial conditions, *Tellus, Ser. B*, **41**, 452–468.
- Johnsen, S. J., D. Dahl-Jensen, W. Dansgaard, and N. Gundestrup (1995), Greenland palaeotemperatures derived from GRIP bore hole temperature and ice core isotope profiles, *Tellus, Ser. B*, **47**, 624–629.
- Johnsen, S. J., et al. (1997), The  $^{18}\text{O}$  record along the Greenland Ice Core Project deep ice core and the problem of possible Eemian climatic instability, *J. Geophys. Res.*, **102**, 26,397–26,410.
- Korte, M., and C. Constable (2005), Continuous geomagnetic field models for the past 7 millennia: 2. CALS7K, *Geochem. Geophys. Geosyst.*, **6**, Q02H16, doi:10.1029/2004GC000801.
- Lal, D., and B. Peters (1967), Cosmic ray produced radioactivity on the Earth, in *Handbuch für Physik*, edited by S. Flügge, pp. 551–612, Springer, New York.
- Lean, J., and D. Rind (1999), Evaluating sun-climate relationships since the Little Ice Age, *J. Atmos. Sol. Terr. Phys.*, **61**, 25–36.
- Lean, J., J. Beer, and R. Bradley (1995), Reconstruction of solar irradiance since 1610: implications for climate change, *Geophys. Res. Lett.*, **22**, 3195–3198.
- Legrand, J. P., and P. A. Simon (1987), Two hundred years of auroral activity (1780–1979), *Ann. Geophys.*, **5a**, 161–168.
- Lockwood, G. W. (1994), Irradiance variations of stars, in *The Sun as a Variable Star: Solar and Stellar Irradiance Variations*, edited by J. M. Pap et al., pp. 20–27, Cambridge Univ. Press, New York.
- Lockwood, M. (2004), Solar outputs, their variations and their effects on Earth, in *Saas-Fee Advanced Course 34: The Sun, Solar Analogs and the Climate*, edited by I. Rüedi, M. Güdel, and W. Schmutz, pp. 109–289, Springer, New York.
- Magny, M. (1993), Solar influences on Holocene climatic changes illustrated by correlations between past lake-level fluctuations and the atmospheric  $^{14}\text{C}$  record, *Quat. Res.*, **40**, 1–9.
- Masarik, J., and J. Beer (1999), Simulation of particle fluxes and cosmogenic nuclide production in the Earth's atmosphere, *J. Geophys. Res.*, **104**, 12,099–13,012.
- Masarik, J., and R. C. Reedy (1994), Effects of bulk chemical composition on nuclide production processes in meteorites, *Geochim. Cosmochim. Acta*, **58**, 5307–5317.
- Mayaud, S. N. (1973), A hundred year series of geomagnetic data 1868–1967. Indices aa, Storm sudden commencements, *Bull. Int. Assoc. Geomagn. Aeron.*, **33**, 1–251.
- Mayewski, P. A., L. D. Meeker, M. S. Twickler, S. Whitlow, Q. Yang, W. B. Lyons, and M. Prentice (1997), Major features and forcing of high-latitude northern hemisphere atmospheric circulation using a 110,000 year-long glaciochemical series, *J. Geophys. Res.*, **102**, 26,345–326,366.
- McCracken, K. G. (2001), Variations in the production of  $^{10}\text{Be}$  due to the 11 year modulation of the cosmic radiation, and variations in the vector geomagnetic dipole, paper presented at ICRC 2001, Copernicus Gesellschaft 2001, Hamburg, Germany.
- McCracken, K. G. (2004), Geomagnetic and atmospheric effects upon the cosmogenic  $^{10}\text{Be}$  observed in polar ice, *J. Geophys. Res.*, **109**, A04101, doi:10.1029/2003JA010060.
- McCracken, K. G., and F. B. McDonald (2001), The long term modulation of the galactic cosmic radiation, 1500–2000, paper presented at ICRC 2001, Copernicus Gesellschaft 2001, Hamburg, Germany.
- McCracken, K. G., F. B. McDonald, J. Beer, G. M. Raisbeck, and F. Yiou (2004), A phenomenological study of the long-term cosmic ray modulation, 850–1958 AD, *J. Geophys. Res.*, **109**, A12103, doi:10.1029/2004JA010685.
- Muscheler, R., J. Beer, G. Wagner, C. Laj, C. Kissel, G. M. Raisbeck, F. Yiou, and P. W. Kubik (2004), Changes in the carbon cycle during the last deglaciation as indicated by the comparison of  $^{10}\text{Be}$  and  $^{14}\text{C}$  records, *Earth. Planet. Sci. Lett.*, **219**, 325–340.
- Muscheler, R., J. Beer, P. W. Kubik, and H.-A. Synal (2005a), Geomagnetic field intensity during the last 60,000 years based on  $^{10}\text{Be}$  &  $^{36}\text{Cl}$  from the Summit ice cores and  $^{14}\text{C}$ , *Quat. Sci. Rev.*, doi:10.1016/j.quascirev.2005.1001.1012.
- Muscheler, R., F. Joos, S. A. Müller, and I. Snowball (2005b), Not so unusual-today's solar activity, *Nature*, **436**, doi:10.1038/nature04045.
- Muscheler, R. F. Joos, J. Beer, S. A. Müller, M. Vonmoos, and I. Snowball (2006), Solar activity during the last 1000 yr inferred from radionuclide records, *Quat. Sci. Rev.*, doi:10.1016/j.quascirev.2006.07.012.
- Neff, U., S. J. Burns, A. Mangini, M. Mudelsee, D. Fleitmann, and A. Matter (2001), Strong coherence between solar variability and the monsoon in Oman between 9 and 6 kyr ago, *Nature*, **411**, 290–293.
- Parker, E. N. (1965), The passage of energetic charged particles through interplanetary space, *Planet. Space Sci.*, **13**, 9–49.
- Radick, R. R., G. W. Lockwood, and S. L. Baliunas (1990), Stellar activity and brightness variations: a glimpse at the Sun's history, *Science*, **247**, 39–247.
- Raisbeck, G. M., F. Yiou, M. Fruneau, J. M. Loiseaux, M. Lieuvain, and J. C. Ravel (1981), Cosmogenic  $^{10}\text{Be}/^{7}\text{Be}$  as a probe of atmospheric transport processes, *Geophys. Res. Lett.*, **8**, 1015–1018.
- Reid, G. C. (1991), Solar total irradiance variations and the global sea surface temperature record, *J. Geophys. Res.*, **96**, 2835–2844.
- Ribes, E., B. Beardsley, T.-M. Brown, P. Delache, F. Laclare, J.-R. Kuhn, and N.-V. Leister (1991), The variability of the solar diameter, in *Sun in Time*, edited by C. Sonnet, M. S. Giampapa, and M. S. Matthews, pp. 59–97, Univ. of Ariz. Press, Tucson.
- Rind, D. (2002), The Sun's role in climate variations, *Science*, **296**, 673–677.

- Shindell, D., G. A. Schmidt, M. E. Mann, D. Rind, and A. Waple (2001), Solar forcing of regional climate change during the Maunder Minimum, *Science*, **294**, 2149–2152.
- Simpson, J. A. (1978), Charged-particle astronomy in the outer solar system, *Astronaut. Aeronaut.*, **16**, 96–105.
- Solanki, S. K., I. G. Usoskin, B. Kromer, M. Schüssler, and J. Beer (2004), Unusual activity of the Sun during recent decades compared to the previous 11,000 years, *Nature*, **431**, 1084–1087.
- Steig, E. J., P. J. Polissar, M. Stuiver, P. M. Grootes, and R. C. Finkel (1996), Large amplitude solar modulation cycles of  $^{10}\text{Be}$  in Antarctica: implications for atmospheric mixing processes and interpretation of the ice core record, *Geophys. Res. Lett.*, **23**, 523–526.
- Stuiver, M., and T. F. Braziunas (1988), The solar component of the atmospheric  $^{14}\text{C}$  record, in *Secular Solar and Geomagnetic Variations in the Last 10,000 Years*, edited by F. R. Stephenson and A. W. Wolfendale, pp. 245–266, Springer, New York.
- Stuiver, M., P. J. Reimer, E. Bard, J. W. Beck, G. S. Burr, K. A. Hughen, B. Kromer, G. McCormac, J. Van der Plicht, and M. Spurk (1998), INTCAL98 Radiocarbon age calibration, 24,000-0 cal BP, *Radiocarbon*, **40**, 1041–1083.
- Suess, H. E. (1953), Natural radiocarbon and the rate of exchange of carbon dioxide between the atmosphere and the sea, in *Natural Radiocarbon and the Rate of Exchange of Carbon Dioxide Between the Atmosphere and the Sea*, edited by National Research Council Committee on Nuclear Science, pp. 52–56, Univ. of Chicago Press, Chicago.
- Usoskin, I. G., K. Alanko, K. Mursula, and G. A. Kovaltsov (2002), Heliospheric modulation strength during the neutron monitor era, *Solar Phys.*, **207**, 389–399.
- Usoskin, I. G., S. K. Solanki, M. Schüssler, K. Mursula, and K. Alanko (2003), A millennium scale sunspot number reconstruction: Evidence for an unusually active Sun since the 1940's, *Phys. Rev. Lett.*, **92**, 211101.
- Van Geel, B., J. Buurman, and H. T. Waterbolk (1996), Archaeological and palaeoecological indications of an abrupt climate change in The Netherlands, and evidence for climatological teleconnections around 2650 BP, *J. Quat. Sci.*, **11**, 451–460.
- Verschuren, D., K. R. Laird, and B. F. Cumming (2000), Rainfall and drought in equatorial east Africa during the past 11,000 years, *Nature*, **403**, 410–414.
- Wagner, G., J. Masarik, J. Beer, S. Baumgartner, D. Imboden, P. W. Kubik, H.-A. Synal, and M. Suter (2000), Reconstruction of the geomagnetic field between 20 and 60 kyr BP from cosmogenic radionuclides in the GRIP ice core, *Nucl. Instrum. Methods Phys. Res., Sect. B*, **172**, 597–604.
- Wagner, G., J. Beer, J. Masarik, R. Muscheler, P. Kubik, W. Mende, C. Laj, G. M. Raisbeck, and F. Yiou (2001), Presence of the solar de Vries cycle ( $\sim$ 205 years) during the last ice age, *Geophys. Res. Lett.*, **28**, 303–306.
- Webber, W. R., and P. R. Higbie (2003), Production of cosmogenic Be nuclei in the Earth's atmosphere by cosmic rays: Its dependence on solar modulation and the interstellar cosmic ray spectrum, *J. Geophys. Res.*, **108**(A9), 1355, doi:10.1029/2003JA009863.
- Webber, W. R., and J. A. Lockwood (2001), Voyager and Pioneer spacecraft measurements of cosmic ray intensities in the outer heliosphere: Toward a new paradigm for understanding the global solar modulation process: 1. Minimum solar modulation (1987 and 1997), *J. Geophys. Res.*, **106**, 29,323–29,331.
- Willson, R. C. (1997), Total solar irradiance trend during solar cycles 21 and 22, *Science*, **277**, 1963–1965.
- Yang, S., H. Odah, and J. Shaw (2000), Variations in the geomagnetic dipole moment over the last 12000 years, *Geophys. J. Int.*, **140**, 158–162.
- Yiou, F., et al. (1997), Beryllium 10 in the Greenland Ice Core Project ice core at Summit, Greenland, *J. Geophys. Res.*, **102**, 26,783–26,794.

J. Beer and M. Vonmoos, Swiss Federal Institute of Environmental Science and Technology, Ueberlandstrasse 133, CH-8600 Dübendorf, Switzerland. (beer@eawag.ch; maura.vonmoos@eawag.ch)

R. Muscheler, Goddard Earth Sciences and Technology Center, University of Maryland Baltimore County, Climate and Radiation Branch, NASA Goddard Space Flight Center, Mail Code 613.2, Greenbelt, MD 20771, USA. (raimund@climate.gsfc.nasa.gov)